

Galaxy Activity in Merging Binary Galaxy Clusters

Ho Seong Hwang^{1*†}, Myung Gyoon Lee²,

¹*School of Physics, Korea Institute for Advanced Study, Seoul 130-722, Korea*

²*Astronomy Program, Department of Physics and Astronomy, FPRD, Seoul National University, Seoul 151-742, Korea*

25 October 2018

ABSTRACT

We present the results of a study of galaxy activity in two merging binary clusters (A168 and A1750) using the Sloan Digital Sky Survey (SDSS) data supplemented with the data in the literature. We have investigated the merger histories of A168 and A1750 by combining the results from a two-body dynamical model and X-ray data. In A168 two subclusters appear to have passed each other and to be coming together from the recent maximum separation. In A1750, two major subclusters appear to have started interaction and to be coming together for the first time. We find an enhanced concentration of the galaxies showing star formation (SF) or active galactic nuclei (AGN) activity in the region between two subclusters in A168, which were possibly triggered by the cluster merger. In A1750, we do not find any galaxies with SF/AGN activity in the region between two subclusters, indicating that two major subclusters are in the early stage of merging.

Key words: galaxies: clusters: general – galaxies: clusters: individual (A168, A1750)

1 INTRODUCTION

In the current models of hierarchical structure formation, clusters of galaxies grow through continuous mergers with groups or clusters. X-ray observations revealed that a significant fraction (40 – 70 per cent) of them show substructures, indicating that they are in the process of merging (e.g., Jones & Forman 1999). There are various evidences for cluster mergers seen in intracluster medium (ICM): complex density and temperature distribution, shocks, and radio halos and relics (e.g., Ricker 1998; Takizawa 2000; Ricker & Sarazin 2001; Buote 2002; Poole et al. 2006; Markevitch & Vikhlinin 2007). It is known that a cluster merger event, which is one of the most extreme phenomena in the universe, releases an enormous amount of energy ($> 10^{63}$ ergs), resulting in several active phenomena. However, the effect of the cluster merger on cluster galaxies is still poorly understood (Girardi & Biviano 2002), and one of the current key questions on clusters is waiting for an answer: does the merging between clusters trigger/suppress star formation (SF) and active galactic nuclei (AGN) activity?

There were several studies to investigate the effect of the cluster merger on cluster galaxies. Caldwell et al. (1993)

found that there is a large fraction of early-type galaxies showing enhanced Balmer absorption lines or emission lines in Coma cluster, indicating the presence of recent SF or nuclear activity. These active galaxies are located at the region between the cluster centre and the subcluster. They extended their study to five other nearby clusters (Caldwell & Rose 1997), and suggested that the merger between the cluster and subcluster may trigger SF in galaxies. Other studies also found evidences for an enhanced galaxy activity possibly triggered by the cluster merger (Burns et al. 1994; Miller & Owen 2003; Cortese et al. 2004, 2006; Ferrari et al. 2005; Johnston-Hollitt et al. 2008).

On the other hand Tomita et al. (1996) found no evidence for enhanced fraction of blue galaxies in the region between two subclusters in a merging cluster A168. Mauduit & Mamon (2007) also found a reduced radio loudness (or reduced AGN/SF activity) of the galaxies in the Shapley Supercluster. This can be explained by the effect of enhanced ram-pressure occurring when galaxies cross the shock front of merging clusters. Recently, Martini, Mulchaey, & Kelson (2007) found that the AGN fraction is the largest in the merging clusters, while De Propriis et al. (2004) found no correlation between the number fraction of blue galaxies and the probability of substructure in clusters.

Numerical simulations also show diverse results. The SF activity during the cluster merger can be triggered by a time-dependent tidal gravitational field of the merging (Bekki 1999), and by an increased ram-pressure of

* E-mail: hshwang@kias.re.kr (HSH); mglee@astro.snu.ac.kr (MGL)

† Present address: CEA, Laboratoire AIM, Irfu/SAP, F-91191 Gif-sur-Yvette, France

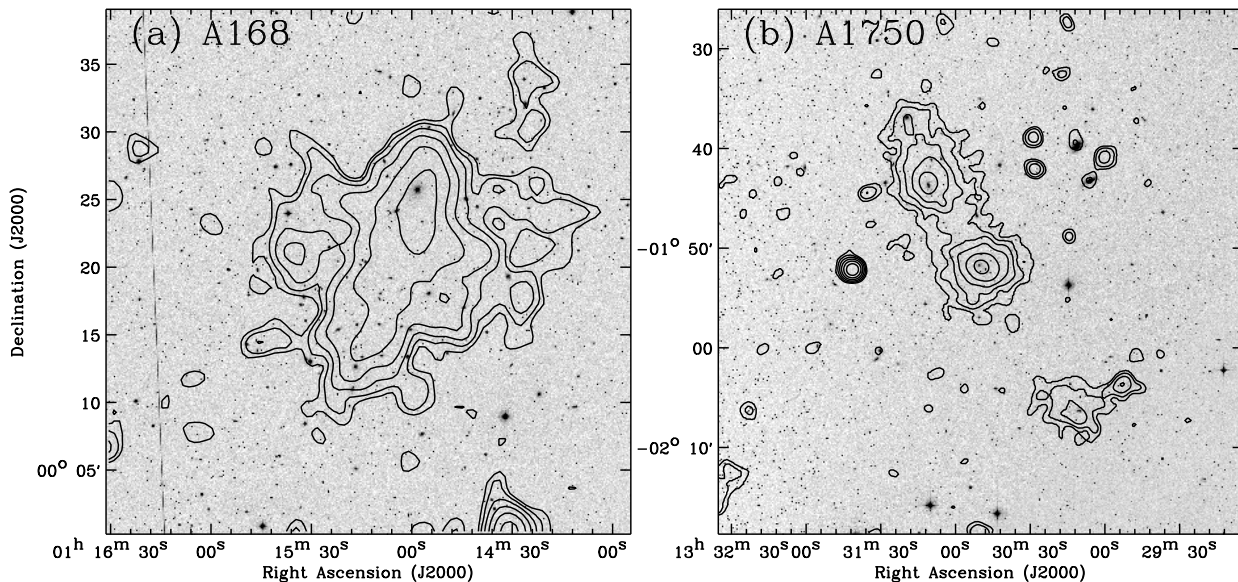


Figure 1. Contours of X-ray intensity overlaid on the optical Digitized Sky Survey for A168 (a) and A1750 (b). X-ray images are taken from EINSTEIN/IPC and ROSAT/PSPC for A168 and A1750, respectively. X-ray contours are smoothed with a Gaussian filter of $\sigma = 31$ arcsec (A168) and 27 arcsec (A1750).

ICM (Kronberger et al. 2008) (see also Gnedin 2003; Kapferer et al. 2006). In contrast the star formation rates of galaxies in the cluster merger can be decreased because of increased ram-pressure (Fujita et al. 1999).

The diverse results of galaxy properties due to the cluster merger might be due to the facts that the clusters are in different merging stages and that the initial conditions of the merging (cluster mass, galaxy morphology, richness of gas, *etc.*) are different. Therefore it is need to study the clusters in various merging stages to understand the effect of the cluster merger on the galaxies in detail. As a first step for the study of galaxy clusters in various merging stages, we focus on two merging binary clusters (A168 and A1750) that are in dynamical state simpler compared to other merging clusters.

A168, shown in Fig. 1(a), is a nearby ($z \sim 0.045$; Struble & Rood 1999) galaxy cluster with BM type II-III. Ulmer, Wirth, & Kowalski (1992) found that there exists an offset between X-ray and optical centres, and suggested that A168 is formed by a collision of two approximately equal sized clusters. Early X-ray images with *Einstein* IPC showed an irregular structure of ICM (Ulmer, Wirth, & Kowalski 1992; Jones & Forman 1999), but recent *Chandra* data revealed two distinguishable X-ray peaks corresponding to the brightest galaxies in each subcluster (Hallman & Markevitch 2004; Yang et al. 2004b). Based on the photometric survey for A168, Tomita et al. (1996) found no evidence for any enhanced fraction of blue galaxies in the cluster region. Using the photometric data from the Beijing-Arizona-Taiwan-Connecticut (BATC) sky survey and the Sloan Digital Sky Survey (SDSS), Yang et al. (2004a) determined the photometric redshifts of galaxies in the region of A168. They secured a sample of 376 probable member galaxies associated with A168, and confirmed the existence of two subclusters corresponding to two X-ray peaks. The two subclusters are separated by $\sim 13.8'$ (~ 510

h^{-1} kpc, where h is the Hubble constant normalized to $100 \text{ km s}^{-1} \text{ Mpc}^{-1}$) on the sky, and show a radial velocity difference of $\sim 260 \text{ km s}^{-1}$. Merger event between the two appears to occur in the plane of the sky, but their merging stage is still debated (Yang et al. 2004a,b; Hallman & Markevitch 2004).

A1750 is a BM type II-III cluster, and is more distant ($z \sim 0.085$; Struble & Rood 1999) compared with A168. In Fig. 1(b), it shows two major X-ray peaks (Forman et al. 1981; Donnelly et al. 2001; Belsole et al. 2004), being known as a canonical binary cluster. However, it also shows another minor X-ray peak to the southwest (Jones & Forman 1999). The spatial distribution of galaxies coincides well with these X-ray peaks (Ramírez & Quintana 1990; Beers et al. 1991; Donnelly et al. 2001). The two subclusters associated with two major X-ray peaks are separated by $\sim 9.6'$ ($\sim 640 h^{-1}$ kpc) on the sky, and have a radial velocity difference of $\sim 1300 \text{ km s}^{-1}$. X-ray data show a weak temperature enhancement (~ 30 per cent) in the region between two subclusters, suggestive of an early stage of merger (Donnelly et al. 2001; Belsole et al. 2004).

In this paper, we investigate the dynamical state and galaxy properties of these two merging binary clusters (A168 and A1750) using the SDSS data supplemented with data in the literature. Section 2 describes the sample of galaxies used in this study. The properties of galaxies in subclusters and dynamical models for the clusters are given in §3. In §4 we discuss the effect of cluster merging on galaxy activity, merging history, and E+A galaxies. Primary results are summarized in the final section. Throughout, we adopt a flat Λ CDM cosmology with density parameters $\Omega_{\Lambda} = 0.73$ and $\Omega_m = 0.27$.

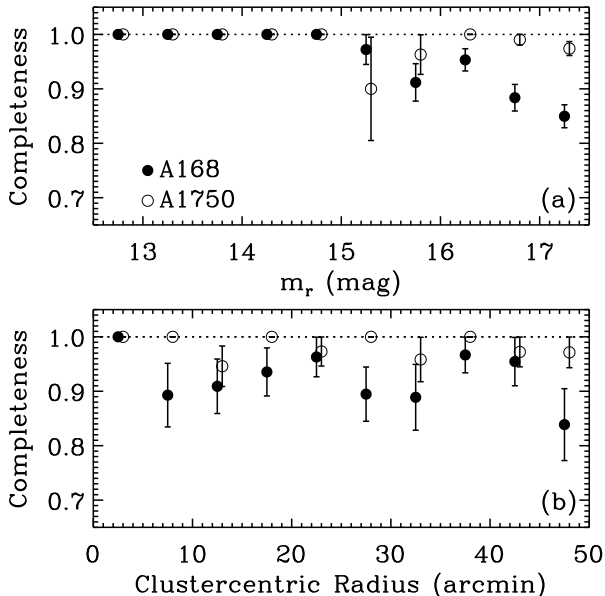


Figure 2. Spectroscopic completeness of the data complemented by NED as a function of r -band magnitude (a) and clustercentric radius (b). Filled and open circles are the completeness for A168 and A1750, respectively. Open circles are slightly shifted to rightwards not to overlap with filled circles.

2 DATA

2.1 Galaxy Sample

We used mainly a spectroscopic sample of galaxies in the Legacy survey of SDSS Sixth Data Release (DR6; Adelman-McCarthy et al. 2008). The Legacy survey contains five-band ($ugriz$) photometric data for 230 million objects over $8,400 \text{ deg}^2$, and optical spectroscopic data more than one million objects of galaxies, quasars, and stars over 6860 deg^2 (Gunn et al. 1998, 2006; Uomoto et al. 1999; Castander et al. 2001; Blanton et al. 2003a; Fukugita et al. 1996; Lupton et al. 2002; Hogg et al. 2001; Smith et al. 2002; Ivezić et al. 2004; Tucker et al. 2006; Pier et al. 2003). Extensive description of SDSS data products is given by York et al. (2000) and Stoughton et al. (2002).

The data is supplemented by several value-added galaxy catalogues (VAGCs) drawn from SDSS data. Photometric and structure parameters are adopted from SDSS pipeline (Stoughton et al. 2002). Complementary photometric parameters such as colour gradient and concentration index are taken from DR4plus sample of Choi, Park, & Vogeley (2007). The spectroscopic parameters are used from MPA/JHU VAGC (Tremonti et al. 2004).

Completeness of the SDSS spectroscopic data is poor for bright galaxies with $m_r < 14.5$ because of the problems of saturation and cross-talk in the spectrograph, and due to the fibre collision for the galaxies located at high density regions such as galaxy clusters (two spectroscopic fibres cannot be placed closer than 55 arcsec on a given plate). Thus, it is needed to supplement the missing galaxy data to reduce the possible effect drawn from the incompleteness problem (e.g., Park & Hwang 2008). We added a photometric sample of galaxies in SDSS ($m_r \leq 18.0$) located within $4 h^{-1} \text{ Mpc}$ from the galaxy cluster, of which redshifts are

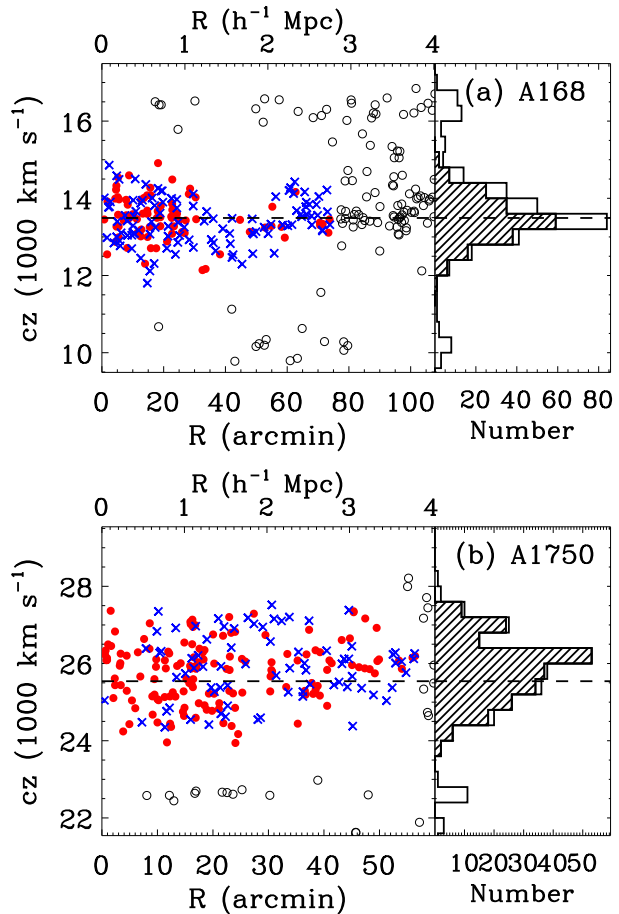


Figure 3. Radial velocity vs. clustercentric distance of galaxies and the velocity distribution for the galaxies in A168 (a) and A1750 (b). Filled circles and crosses, respectively, indicate early- and late-type galaxies selected as cluster members, while open circles denote those that were not selected as cluster members. The horizontal dashed lines indicate the systemic velocity of the clusters adopted from Struble & Rood (1999). The velocity distributions for the member galaxies are shown by hatched histograms, and those for all of the observed galaxies by open histograms.

available at the NASA Extragalactic Database (NED). Figure 2 shows the spectroscopic completeness of our galaxy sample complemented by NED as a function of apparent magnitude and of clustercentric distance. It shows that the spectroscopic completeness of our sample is higher than 85% at all magnitudes and clustercentric radii.

The r -band absolute magnitude M_r was computed using the formula,

$$M_r = m_r - DM - K(z) - E(z), \quad (1)$$

where DM is a distance modulus, $K(z)$ is a K -correction, and $E(z)$ is a luminosity evolution correction. DM is defined by $DM \equiv 5 \log(D_L/10)$ and D_L is a luminosity distance in unit of pc. The rest-frame absolute magnitudes of individual galaxies are computed in fixed bandpasses, shifted to $z = 0.1$, with the Galactic reddening correction (Schlegel, Finkbeiner, & Davis 1998) and the K -correction as described by Blanton et al. (2003b). The evolution correction given by Tegmark et al. (2004), $E(z) = 1.6(z - 0.1)$, is also applied. The $^{0.1}(u-r)$ colour was computed using the

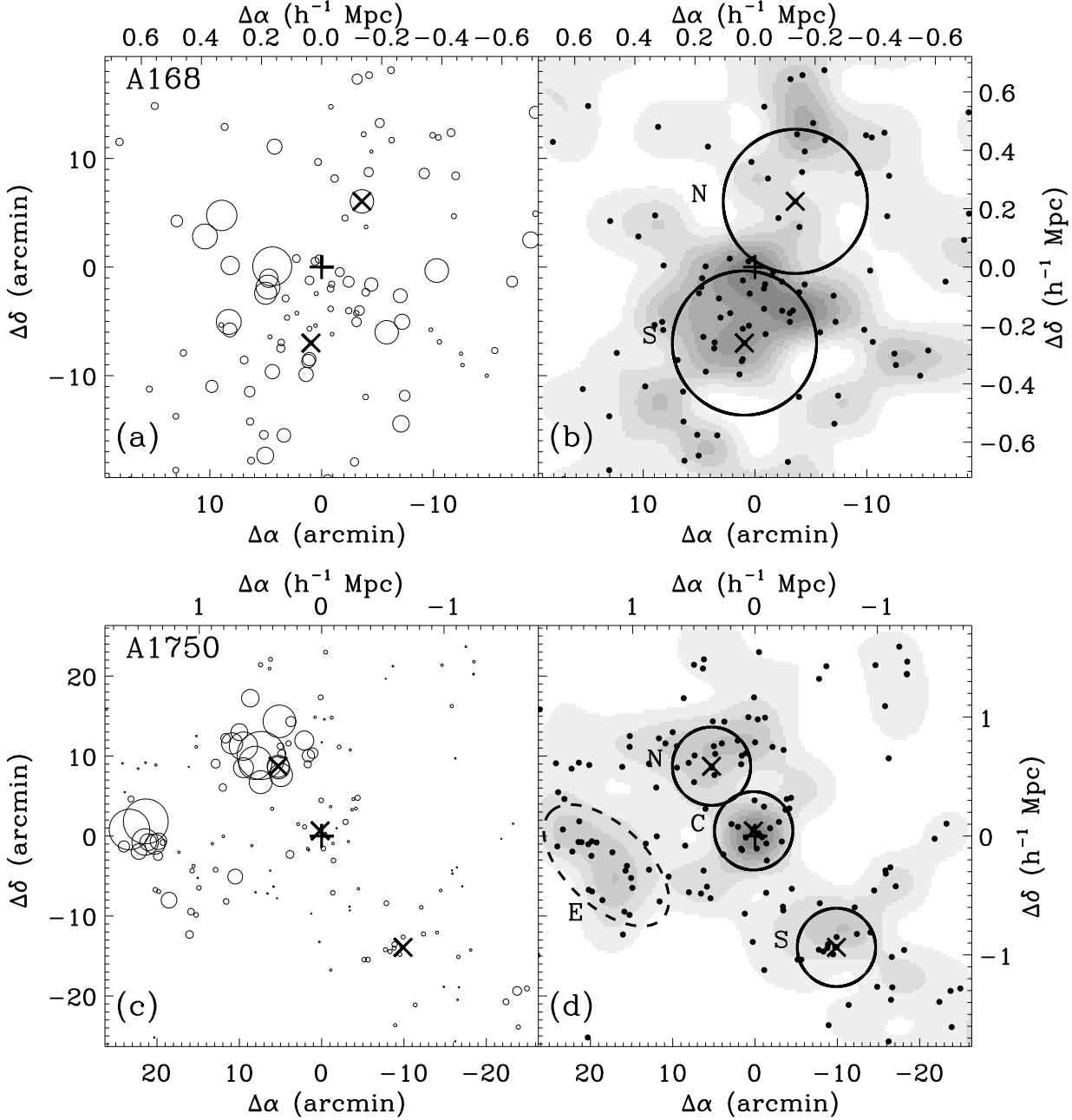


Figure 4. *Left panels:* Dressler-Shectman (DS) plots for A168 (a) and A1750 (c). Each galaxy is plotted by a circle with diameter proportional to e^{δ} . Plus sign indicates the cluster centre we adopted. Crosses indicate the brightest galaxies in the subclusters represented by large circles in right panels. North is up, and east is to the left. *Right panels:* Spatial distribution of cluster galaxies (dots) overlaid on the galaxy number density maps for A168 (b) and A1750 (d). The galaxy number density maps are constructed using the member galaxies with $m_r \leq 17.77$ mag. Radii of the solid circles that define the subclusters are 240 and 320 h^{-1} kpc for A168 and A1750, respectively. Galaxies within a dashed ellipse in (d) will be discussed in §4.2.

model magnitudes with extinction and K -corrections. The superscript 0.1 means the rest-frame magnitude K -corrected to the redshift of 0.1, and will subsequently be dropped.

First we classify the morphological types of galaxies included in DR4plus sample of Choi, Park, & Vogeley (2007) adopting the method given by Park & Choi (2005). Galaxies are divided into early (ellipticals and lenticulars) and late (spirals and irregulars) morphological types based on their

locations in the $(u-r)$ colour versus $(g-i)$ colour gradient space and also in the i -band concentration index space. The resulting morphological classification has completeness and reliability reaching ~ 90 per cent. We performed an additional visual check of the colour images of galaxies to correct misclassifications by the automated scheme. In addition, for the galaxies in DR6 that were not included in DR4plus sam-

ple ($\sim 35\%$), we visually classified the morphological types using the colour images.

2.2 Cluster Membership

To determine the membership of galaxies in a cluster, we used the ‘shifting gapper’ method of Fadda et al. (1996) that was used for the study of kinematics of galaxy clusters (Hwang & Lee 2007, 2008). In the radial velocity versus clustercentric distance space, the cluster member galaxies are selected by grouping galaxies with connection lengths of 950 km s^{-1} in the direction of the radial velocity and of $0.1 h^{-1} \text{ Mpc}$ in the direction of the clustercentric radius R . If there are no adjacent galaxies with $> 0.1 h^{-1} \text{ Mpc}$, we stopped the procedure. The boundary for the member galaxies is different depending on the cluster (see Fig. 3). We iterated the procedure until the number of cluster members is converged. Fig. 3 shows plots of radial velocity as a function of clustercentric distance of galaxies, and the velocity distributions for the galaxies in A168 and A1750.

3 RESULTS

3.1 Substructure

To find the dynamical state of our sample clusters, we first identify the subclusters in the clusters. Using the velocity data and positional information on the galaxies, we performed a Δ -test (Dressler & Shectman 1988), which computes local deviations from the systemic velocity (v_{sys}) and velocity dispersion ($\sigma_{\text{cl,all}}$) of the entire cluster. For each galaxy, the deviation is defined by

$$\delta^2 = \frac{N_{nn}}{\sigma_{\text{cl,all}}^2} [(v_{\text{local}} - v_{\text{sys}})^2 + (\sigma_{\text{local}} - \sigma_{\text{cl,all}})^2], \quad (2)$$

where N_{nn} is the number of the nearest galaxies that defines the local environment, taken to be $N_{\text{gal}}^{1/2}$ in this study. N_{gal} is a total number of member galaxies in the cluster. The nearest galaxies are those located closest to the galaxy on the sky. v_{local} and σ_{local} are systemic velocity and its dispersion estimated from N_{nn} nearest galaxies, respectively.

We plot the positions of cluster galaxies, represented by circles with radii proportional to e^δ , in the left panels of Fig. 4. A large circle denotes a galaxy for which local environment is deviant in either velocity or dispersion compared with the entire cluster. It implies that the groups of large circles indicate the presence of substructure. In A168, two X-ray peaks appear not to be associated with the groups of large circles, while the region between the two X-ray peaks corresponds to a group of large circles along the direction perpendicular to the line connecting two peaks. For A1750, there is seen a strong clustering of large circles to the northeast of the cluster centre, showing clearly that it is a subcluster.

We show the spatial distribution of all member galaxies in the right panels of Fig. 4, where we overlaid the galaxy number density contour map constructed using the bright member galaxies with $m_r \leq 17.77$ mag. It is noted that the galaxy number density is the highest in the region between two X-ray peaks. We identified the brightest galaxies in the subclusters that are roughly matched to X-ray peaks. Then, we secured the subsample of galaxies associated with the

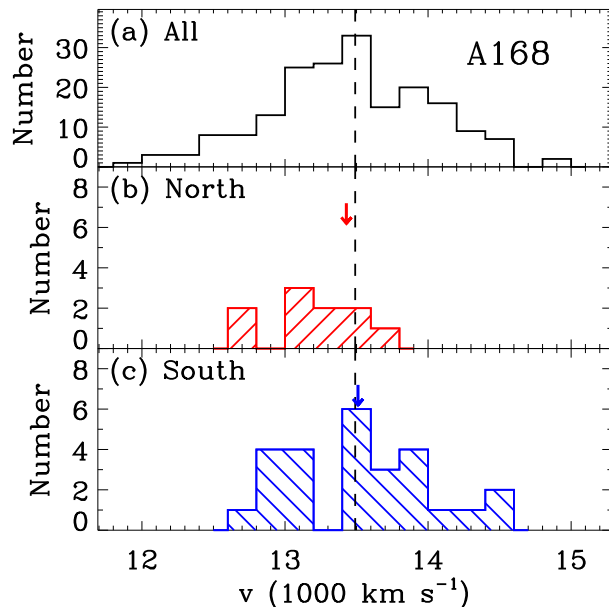


Figure 5. Velocity histogram for all member galaxies in A168 (a), the northern subcluster (b), and the southern subcluster (c). Radial velocity for the brightest galaxy in each subcluster is indicated by a down arrow, and the systemic velocity of A168 is indicated by a vertical dashed line.

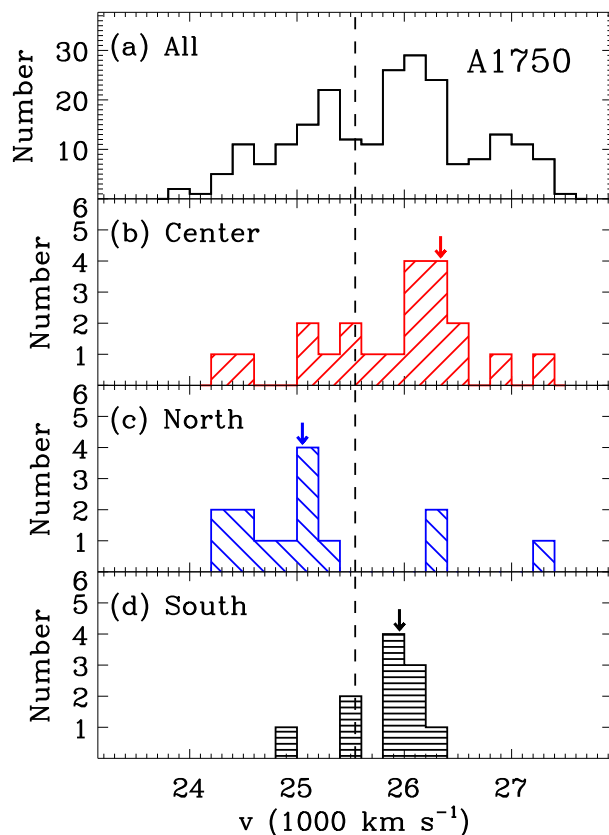


Figure 6. Same as Fig. 5, but for A1750.

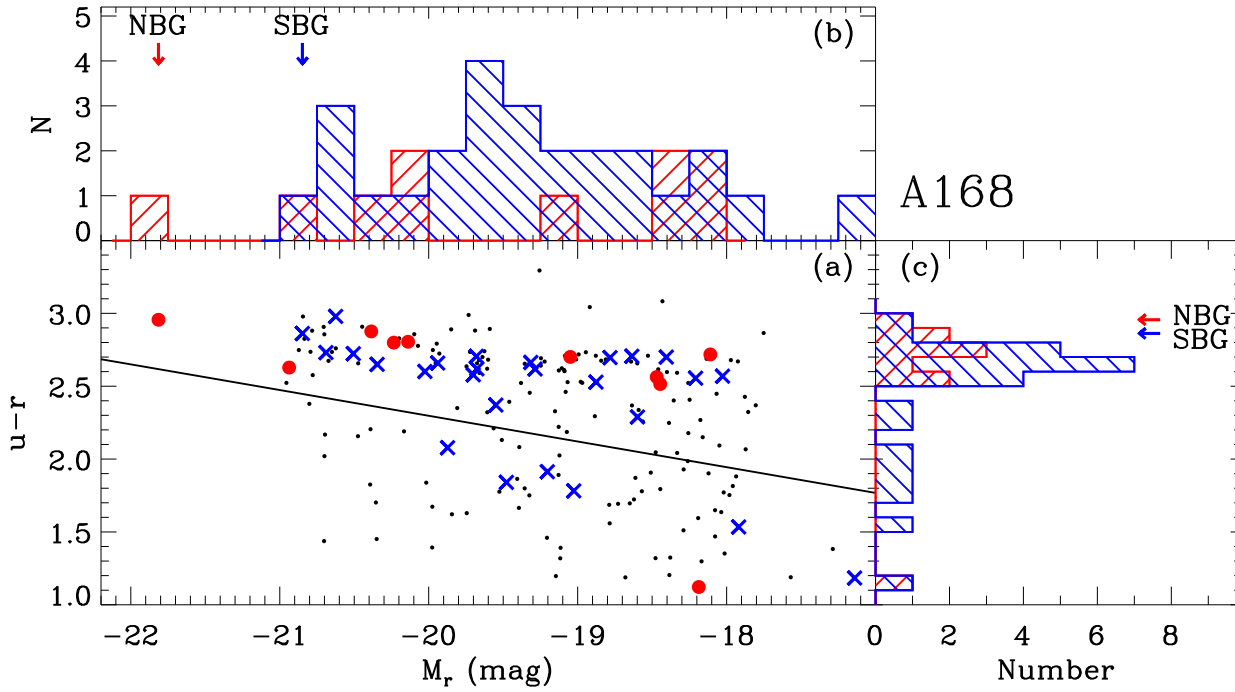


Figure 7. Colour-magnitude diagram and histograms for the galaxies in A168 (a). All member galaxies are indicated by dots, those in A168 N by circles, and those in A168 S by crosses. Solid straight line is the division line for blue and red galaxies given by Choi, Park, & Vogeley (2007). Histograms of absolute magnitudes M_r of galaxies in subclusters (b) and those of $(u-r)$ colours of galaxies in subclusters (c). Galaxies in A168 N and S are denoted by hatched histograms with orientation of 45° (//) and of 315° (\), respectively. The brightest galaxy in each subcluster is indicated by an arrow.

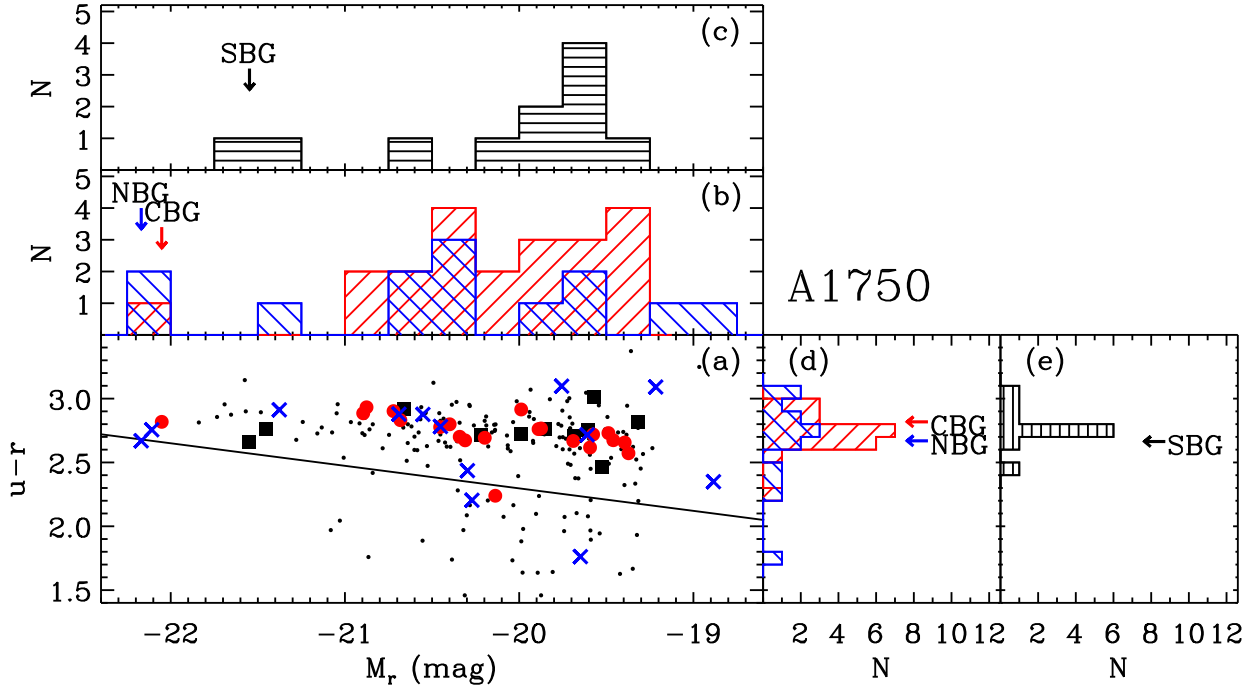


Figure 8. Colour-magnitude diagram and histograms for the galaxies in A1750 (a). All member galaxies are indicated by dots, those in A1750 C by circles, those in A1750 N by crosses, and those in A1750 S by squares. Solid straight line is the division line for blue and red galaxies given by Choi, Park, & Vogeley (2007). Histograms of absolute magnitude M_r for the galaxies in A1750 C and N (b), and those in A1750 S (c). Histograms of $(u-r)$ colours for the galaxies in A1750 C and N (d), and those in A1750 S (e). Galaxies in A1750 C and N are denoted by hatched histograms with orientations of 45° (//) and of 315° (\), respectively. Galaxies in A1750 S are denoted by hatched histograms with orientations of 0° (=). The brightest galaxy in each subcluster is indicated by an arrow.

Table 1. Kinematics for Subclusters

Subsample	N_{gal}	\overline{cz} (km s ⁻¹)	σ_p (km s ⁻¹)	M_{vir} (10 ¹⁴ h ⁻¹ M _⊙)
A168	189	13456 ⁺⁴⁰ ₋₄₃	575 ⁺²⁶ ₋₂₈	
A168 N	10	13214 ⁺¹²³ ₋₉₅	333 ⁺⁶¹ ₋₈₁	0.374 ^{+0.128} _{-0.165}
A168 S	26	13543 ⁺¹⁰⁴ ₋₁₁₁	532 ⁺⁷¹ ₋₆₂	0.752 ^{+0.211} _{-0.141}
A1750	224	25836 ⁺⁵⁶ ₋₅₅	837 ⁺³¹ ₋₃₂	
A1750 C	21	25931 ⁺²¹² ₋₂₀₁	758 ⁺¹⁵¹ ₋₁₆₂	1.696 ^{+0.570} _{-0.593}
A1750 N	14	24999 ⁺²⁶⁰ ₋₁₇₂	791 ⁺³⁵² ₋₂₇₂	2.282 ^{+2.089} _{-1.164}
A1750 S	11	25919 ⁺⁷² ₋₁₁₃	368 ⁺¹⁷⁶ ₋₁₃₉	0.303 ^{+0.294} _{-0.178}

Column descriptions. Column (1): subsamples. Column (2): number of galaxies. Column (3): systemic velocity of the subsamples (biweight location of Beers et al. 1990). Column (4): velocity dispersion of the subsamples (biweight scale of Beers et al. 1990). Column (5): virial mass computed from eq. (4) in Girardi et al. (1998).

subclusters by selecting the galaxies within the circles centred on the brightest galaxies. The radius of the circle for galaxy selection is chosen to contain galaxies as much as possible without overlapping each other. The radius of the circle for A168 is slightly reduced not to contain the galaxies in the other subcluster. Radii of the circles for galaxy selection are 240 and 320 h⁻¹ kpc for A168 and A1750, respectively.

In Figs. 5 and 6, we plot the velocity distributions for the galaxies in the subclusters in company with that for all member galaxies. Table 1 summarizes the kinematic properties of the galaxies in the subclusters. For A168, the relative radial velocity between two subclusters is 330 km s⁻¹, and A168 S appears to be about twice massive than A168 N. For A1750, the mean velocity of A1750 N is significantly different from those of other subclusters as seen in the Dressler-Schechter plot of Fig. 4(c). The masses of A1750 C and N are comparable within the uncertainty, and the mass of A1750 S is the smallest among the subclusters. The velocity distributions for the subclusters show a prominent peak and the velocity dispersions for the subclusters are consistent with the measurements in the previous studies (Yang et al. 2004a; Beers et al. 1991), indicating that they are genuine subclusters.

We present a colour-magnitude diagram for the cluster galaxies in Figs. 7 (A168) and 8 (A1750). The galaxies in the subclusters are represented by different symbols. It is seen that most of the galaxies in the subclusters follow the red sequence in the sense that the brighter galaxies are likely to be redder than the fainter galaxies. However, some galaxies in A168 S show bluer colours than the division line for blue and red galaxies (Choi, Park, & Vogeley 2007), which may indicate SF activity.

3.2 Two-body Dynamical Model

To obtain a hint of merging histories for our sample clusters, we apply a two-body analysis introduced by Beers, Geller, & Huchra (1982). It is assumed that two subclusters have radial orbits: neither shear nor net rotation of the system. It is also assumed that the subclusters are now

moving apart from the zero separation at $t = 0$, or are coming together for the first time. Then the equation of motion for this system is given by,

$$R = \frac{R_p}{\cos \alpha} = \frac{R_m}{2}(1 - \cos \chi), \quad (3)$$

$$V = \frac{V_r}{\sin \alpha} = \left(\frac{2GM_{\text{tot}}}{R_m} \right)^{1/2} \frac{\sin \chi}{(1 - \cos \chi)}, \quad (4)$$

$$t = t_0 = \left(\frac{R_m^3}{8GM_{\text{tot}}} \right)^{1/2} (\chi - \sin \chi), \quad (5)$$

where R is a separation between two subclusters, R_p is a projected separation of the subclusters, α is a projection angle that is an angle between the line connecting two subclusters and the plane of the sky (see Fig. 7 in Beers, Geller, & Huchra 1982 for geometry), R_m is a separation of the subclusters at maximum expansion, and χ is a developmental angle. V is a relative velocity between two subclusters, and V_r is a radial relative velocity between the two. M_{tot} is a total mass of the system, and t is the present time adopted as the age of the universe, $3.064 \text{ h}^{-1} \times 10^{17} \text{ s} = 9.715 \text{ h}^{-1} \text{ Gyr}$ with $\Omega_\Lambda = 0.73$ and $\Omega_m = 0.27$.

The two subclusters have a zero separation at $\chi = 0, 2\pi$, while they are at the maximum expansion at $\chi = \pi, 3\pi$. The solutions with $0 < \chi < 2\pi$ indicate that two subclusters are now moving apart since $t = 0$ with zero separation, or coming together for the first time in their history. On the other hand, the solutions with $2\pi < \chi < 4\pi$ mean that they already experienced one close encounter. In addition, simple Newtonian criterion for the gravitational binding is described by,

$$V_r^2 R_p \leq 2GM_{\text{tot}} \sin^2 \alpha \cos \alpha. \quad (6)$$

In Table 2, we summarised the input and output parameters of the two-body dynamical models for our sample clusters. In Fig. 9, we plot the projection angle α as a function of the radial velocity between two subclusters given by two-body models.

Fig. 9(a) shows that two subclusters in A168 are likely to be a gravitationally bound system unless the projection angle α is smaller than 4°. We investigated two cases of moving apart or coming together for the first time ($0 < \chi < 2\pi$) and experiencing one encounter ($2\pi < \chi < 4\pi$). Since previous studies suggest that subclusters in A168 have already passed each other at least once (Hallman & Markevitch 2004; Yang et al. 2004b), we focus on the solutions with $2\pi < \chi < 4\pi$. For the cases of BO_e and BI_g, the relative velocities V between two subclusters are larger than the velocity dispersion of each subcluster. In addition, since their separation is small ($R \sim 0.52 \text{ h}^{-1} \text{ Mpc}$), it is expected to see merging features such as shocks or strong temperature variations in the region between two subclusters. However, X-ray data do not show such features (Hallman & Markevitch 2004; Yang et al. 2004b), which implies that these solutions are less probable.

For the cases of BO_d and BI_f, two subclusters are separated by $\sim 1.6 \text{ h}^{-1} \text{ Mpc}$ with large projection angles. Case BO_d is an outgoing solution in which the last encounter occurred $\sim 3.1 \text{ h}^{-1} \text{ Gyr}$ ago and two subclusters will move apart for another $0.3 \text{ h}^{-1} \text{ Gyr}$. On the other hand, Case BI_f indicates that two subclusters experienced the last encounter $\sim 3.5 \text{ h}^{-1} \text{ Gyr}$ ago, and reached the

Table 2. Two-body Model Parameters

System (1)	M_{sys} (2)	V_r (3)	R_p (4)	Range (5)	Solution (6)	α (7)	V (8)	R (9)	R_{max} (10)				
A168 N/S	1.13	81 ± 87	0.51	$0 < \chi < 2\pi$	BO _a	82.3	81.7	3.84	3.95				
					BI _b	80.0	82.2	2.96	3.03				
					BI _c	3.9	1197.7	0.52	2.17				
				$2\pi < \chi < 4\pi$	BO _d	72.0	85.2	1.66	1.66				
					BO _e	3.9	1190.7	0.52	2.09				
					BI _f	70.8	85.8	1.56	1.58				
					BI _g	4.3	1082.6	0.52	1.37				
				A1750 N/C	3.98	932 ± 332	0.64	$0 < \chi < 2\pi$	BO _a	86.0	934.3	9.12	...
									BI _b	67.9	1005.9	1.71	3.45
BI _c	29.4	1897.2	0.74						3.30				
$2\pi < \chi < 4\pi$	BO _d	66.0	1019.9					1.58	3.05				
	BO _e	29.6	1885.5					0.74	3.19				
	BI _f	58.1	1098.0					1.22	2.13				
	BI _g	34.1	1663.1					0.78	2.08				

Column descriptions. Column (1): system for two-body model. Column (2): total mass of the system ($10^{14} h^{-1} M_{\odot}$). Column (3): relative radial velocity (km s^{-1}). Column (4): projected separation of two subclusters (h^{-1} Mpc). Column (5): range of χ . Column (6): allowed solutions (BO: Bound-Outgoing case, BI: Bound-Incoming case). Column (7): projection angle (deg). Column (8): relative velocity (km s^{-1}). Column (9): separation of two subclusters (h^{-1} Mpc). Column (10): maximum separation of two subclusters (h^{-1} Mpc).

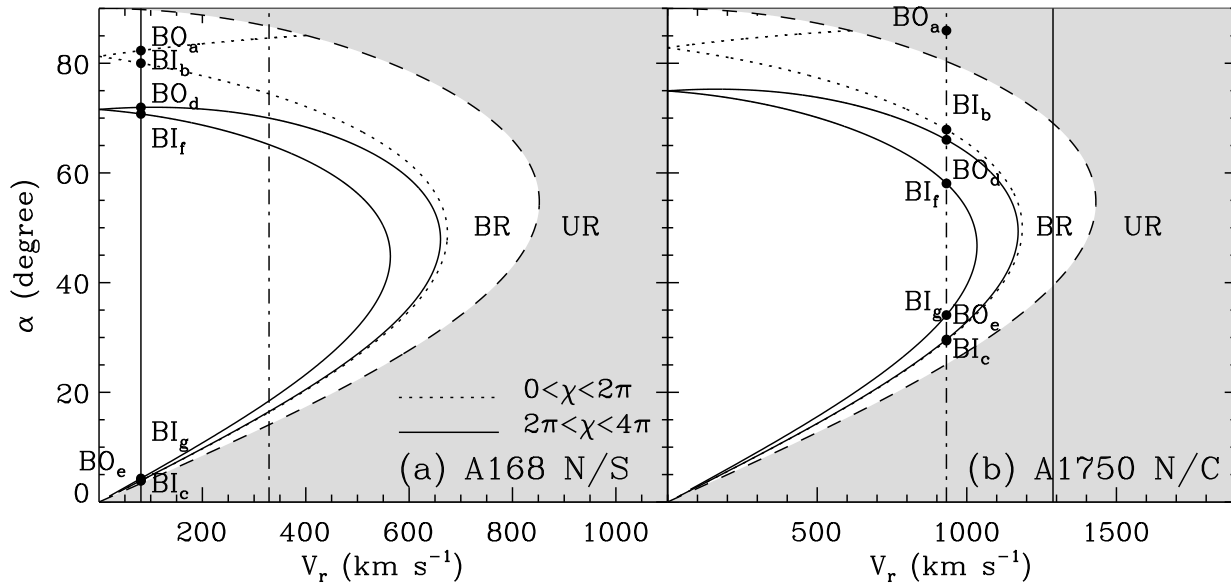


Figure 9. Projection angle α vs. radial velocity difference V_r given by the two-body model for A168 N and S (a) and for A1750 N and C. Filled circles indicate the solutions summarised in Table 2. Solid curved lines are for the case $0 < \chi < 2\pi$, while dotted curved lines for the case $2\pi < \chi < 4\pi$. Vertical solid and dot-dashed lines denote the radial velocity difference for two brightest galaxies in the subclusters and for mean radial velocities of two subclusters, respectively. UR and BR, respectively, indicate unbound (shaded) and bound (clean) region.

maximum expansion of $1.58 h^{-1}$ Mpc about $0.4 h^{-1}$ Gyr ago. Previous *Chandra* data provide us with detailed X-ray image, which is helpful for determining the dynamical state of A168 (Hallman & Markevitch 2004; Yang et al. 2004b). Yang et al. (2004b) reported that X-ray morphology of A168 is similar to that of an off-axis merger with a mass ratio from 1:1 to 1:3 several Gyrs after a core pas-

sage. Hallman & Markevitch (2004) found a cold front at the northern tip of A168 N that is seen for the subcluster at its apocenter (Mathis et al. 2005), and suggested that the two subclusters are in the process of turning around. These X-ray studies are consistent with the solutions of BO_d and BI_f, but BI_f is favoured because of the existence of the northern cold front.

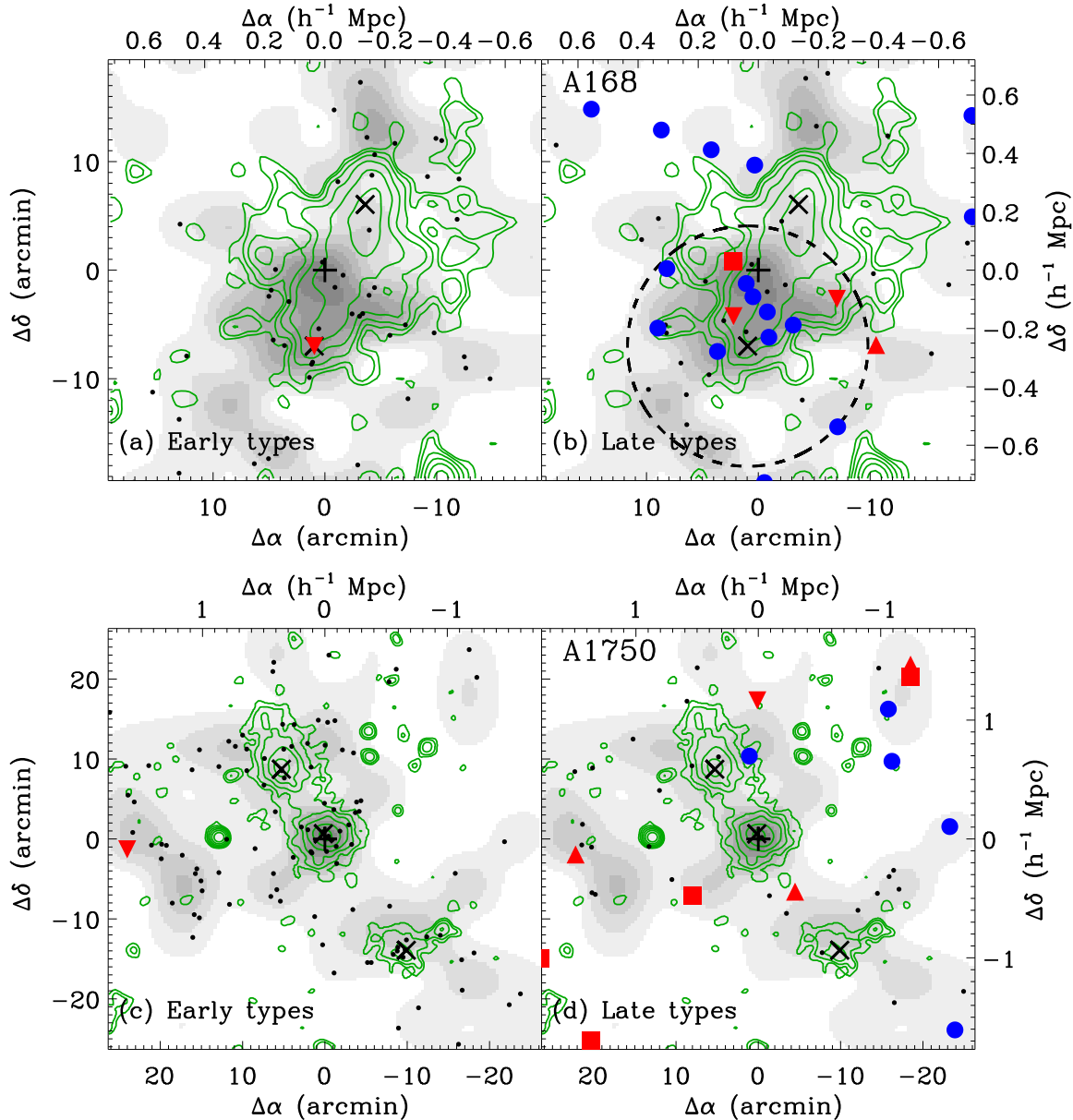


Figure 10. Spatial distribution of early-type (*Left*) and late-type (*Right*) galaxies in clusters on the galaxy number density maps. Contours of X-ray intensity in Fig. 1 are overlaid. Normal galaxies are indicated by dots, while the emission-line galaxies are denoted by various symbols (star-forming galaxies: circles, Seyferts: triangles, LINERs: upside-down triangles, and composite galaxies: squares). Plus sign indicates the centre we adopted, and crosses indicate the brightest galaxies in the subclusters. North is up, and east is to the left. Dashed circle in (b) represents the region that we investigate in Fig. 11.

A1750 is a typical example of merging binary clusters, which has two major subclusters, northern (N) and central (C) subclusters. However, previous studies revealed that there is another subcluster to the south (S), which might be related to the northern and central subclusters (Beers et al. 1991; Jones & Forman 1999). Therefore, two-body model may not be applicable to this cluster. Since the mass of A1750 S is much smaller compared to A1750 N and C, we are going to apply the two-body model to A1750 N and C, and discuss the effect of A1750 S in §4.2. For the two-body model of A1750 N and C, when we use the relative radial velocity between the two brightest galaxies in subclusters

($V_r = 1288 \text{ km s}^{-1}$), we cannot find acceptable solutions in the bound region. When we use the relative radial velocity between the two subclusters computed from average value of galaxy velocities ($V_r = 383 \text{ km s}^{-1}$), we can obtain several bound solutions. Since the X-ray images show weak enhancement in the region between the two subclusters, indicating that the interaction between the two has just started (Belsole et al. 2004), we focus on the incoming solutions with $0 < \chi < 2\pi$.

There are two incoming solutions of BI_b and BI_c with different relative velocity and distance. The BI_c solution has the parameters with the relative velocity of 1897 km s^{-1}

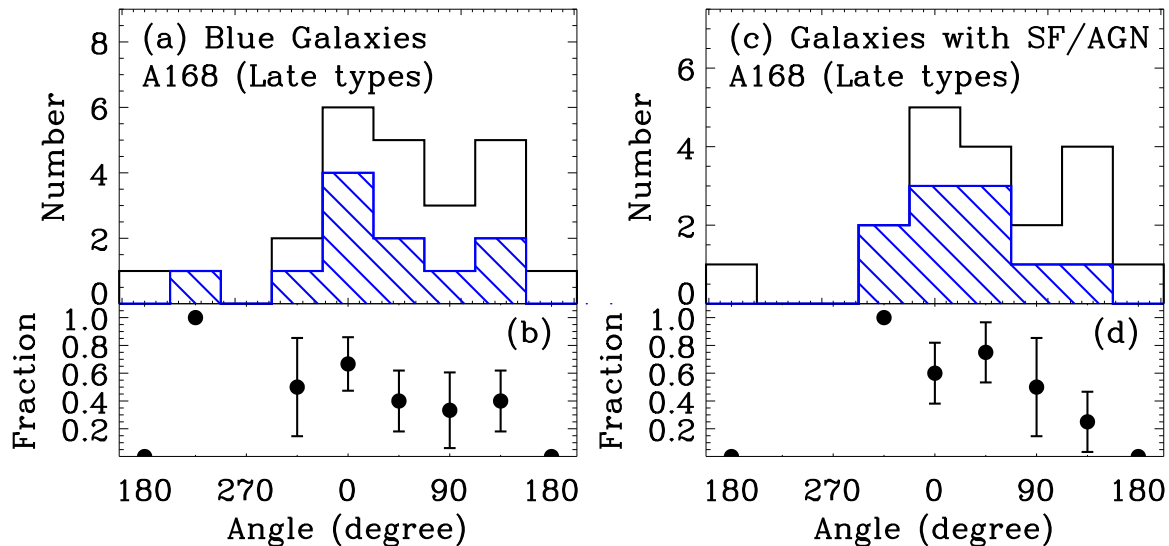


Figure 11. Angular variation of the fraction of blue galaxies (a, b), and that of galaxies with SF/AGN activity (c, d) in A168. Open histogram in (a) is for all the late-type galaxies having $(u - r)$ colour information, and that in (c) is for those having spectral line measurement in A168. Shaded one is for the late-type galaxies with blue colour (a) or with SF/AGN activity (c).

and the separation of $0.74 h^{-1}$ Mpc. Thus, it is expected to see significant surface brightness distortions and temperature enhancement in the region between the two subclusters. However, detailed X-ray data show insignificant distortion of surface brightness and weak enhancement in temperature for that region (Belsole et al. 2004). Therefore, the BI_b solution is more favoured because of the smaller relative velocity and the larger separation of the subclusters compared to the BI_c solution. According to the BI_b solution, the two subclusters will cross each other in about $3.5 h^{-1}$ Gyr.

3.3 Galaxy Activity

In Fig. 10, we show the spatial distribution of all member galaxies divided by their morphologies and spectral types. We determined the spectral types of emission-line galaxies based on the criteria given by Kewley et al. (2006) using the emission line ratio diagram, commonly known as Baldwin-Phillips-Terlevich (BPT) diagram (Baldwin, Phillips, & Terlevich 1981): star-forming galaxies, Seyferts, LINERs, and composite galaxies. Fig. 10 shows that emission-line galaxies among the early-type galaxies in A168 are rarely seen. On the other hand, a significant fraction of late-type galaxies are identified as active ones, and they get together in the region between two subclusters. The two dimensional Kolmogorov-Smirnov test (Fasano & Franceschini 1987) yields that the spatial distributions of emission-line and quiescent galaxies among late types are different with the significance level of 89 per cent.

Previously, Tomita et al. (1996), using a photometric sample of 143 galaxies including 22 galaxies with measured velocities, found no evidence of any enhanced fraction of blue galaxies in the region between two subclusters of A168. To check this result with our data, we plot, in Fig. 11, an angular variation of the fraction of blue galaxies (a, b), and that of galaxies with SF/AGN activity (c, d). Blue galaxies are those whose $(u - r)$ colours are bluer than the divi-

sion line given by Choi, Park, & Vogeley (2007) as shown in Figs. 7 and 8. The division line indicates the lower limit of $(u - r)$ colour dispersion in the colour-magnitude relation of early-type galaxies, which was determined by an eyeball fit (see Fig. 3 in Choi, Park, & Vogeley 2007). The galaxies with SF/AGN activity are those whose spectral types were determined in the BPT diagram (e.g., star-forming galaxies, Seyferts, LINERs, or composite galaxies). The angle is measured counterclockwise centred on the brightest galaxy in A168 S, and 0 degree corresponds to a line connecting the brightest galaxies in A168 S and N. We used the galaxies whose projected distance to the brightest galaxy in A168 S is smaller than $400 h^{-1}$ kpc (shown as the dashed circle in Fig. 10b) and whose absolute magnitude is brighter than $M_r - 18$ mag.

Fig. 11(a, b) shows no enhanced concentration of blue galaxies along the line between the two subclusters ($315^\circ - 45^\circ$), which is consistent with the result given by Tomita et al. (1996). However, Fig. 11(c, d) clearly shows an enhanced concentration of the galaxies with SF/AGN activity along the line between the two subclusters ($315^\circ - 45^\circ$). In A1750, there are few galaxies in the region between A1750 C and N, and there are few emission-line galaxies associated with subclusters.

4 DISCUSSION

4.1 Effect of Cluster Merging on Galaxy Activity in A168

We found that the two subclusters in A168 appear to have experienced last encounter about $3.5 h^{-1}$ Gyr ago, and to be now coming together from the maximum expansion of $1.58 h^{-1}$ Mpc about $0.4 h^{-1}$ Gyr ago. It is needed to check the validity of the assumptions of two-body models (e.g., merging with no angular momentum). If the merging between two subclusters occurs with angular momentum (e.g.,

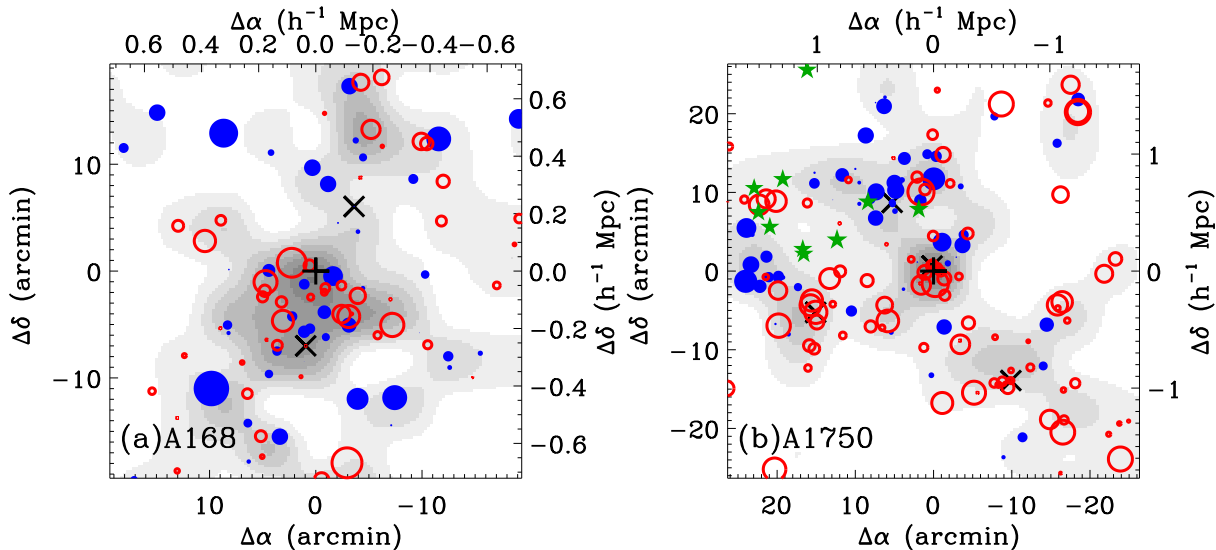


Figure 12. Spatial distribution of the cluster galaxies overlaid on the galaxy number density maps for A168 (a) and A1750 (b). Open circles represent the cluster galaxies whose velocities are greater than the systemic velocity of their cluster, while filled symbols represent those whose velocities are smaller than the systemic velocity. The symbol size is proportional to the velocity deviation from the systemic velocity of the cluster. In A1750 (b), star symbols represent the galaxies with radial velocities of $cz \sim 22,500 \text{ km s}^{-1}$ that show a large velocity deviation ($cz - \bar{cz} \sim -3000 \text{ km s}^{-1}$) from the main body. Plus sign indicates the centre we adopted, and crosses indicate the brightest galaxies in the subclusters. North is up, and east is to the left.

off-axis merger), the observed X-ray brightness will be distorted along the orbital motion as shown in the simulated one (e.g., Fig. 6 in Poole et al. 2006). However, the observed *Chandra* X-ray image of A168 is similar to the case with low angular momentum in the simulated one, which supports our assumption of radial orbits in two-body model for A168.

We found no enhanced concentration of blue galaxies at the region between the two subclusters in A168, which is consistent with the result in Tomita et al. (1996). There are 55 galaxies in common between this study and Tomita et al. (1996), if we use a matching tolerance of $15''$. Among 55 galaxies, 48 galaxies are found to be genuine cluster galaxies associated with A168 when we use the velocity information provided by SDSS and NED. Namely, the photometric sample of galaxies in Tomita et al. (1996) includes about 87 per cent of genuine cluster galaxies associated with A168. In the sample of 48 genuine cluster galaxies associated with A168, we find that the colour types of 42 galaxies are assigned consistently, which leads to the similar finding in both studies [i.e., red (blue or semi-blue) galaxies determined in Tomita et al. (1996) are classified as red (blue) galaxies in this study].

When we use the emission-line diagnostics to detect galaxy activity, we find an enhanced concentration of the galaxies with SF/AGN activity at the region between the two subclusters in A168 (see Figs. 10b and 11d). Emission-line diagnostics is more sensitive to probe SF/AGN activity compared to the integrated colour (Kennicutt 1998; Park & Choi 2009) so that we could directly detect galaxy activity that was not found previously. Considering the morphology-density relation the existence of the late-type galaxies with SF/AGN activity in the region between two subclusters of A168 seems to be caused by some events such as the cluster merger or interaction. The existence of the

galaxies with SF/AGN activity in the region between two subclusters could be also a result of overlapping of the outskirts of two subclusters located at slightly different distance along the line of sight. If so, it is expected that there will be no angular variation of the fraction of the galaxies with SF/AGN activity as shown in Fig. 11. However, Fig. 11(c, d) clearly shows an enhanced concentration of the galaxies with SF/AGN activity along the line between the two subclusters ($315^\circ - 45^\circ$), implying that this scenario is less probable.

4.2 Merging History of A1750

Two major subclusters (A1750 C and N) appear to have started interaction and to be coming together for the first time. In A1750, there are few galaxies in the region between A1750 C and N, and there are few emission-line galaxies associated with subclusters. This indicates that the current merger event started recently, not yet triggering any activity in cluster galaxies.

Detailed *XMM-Newton* images of A1750 C imply that it underwent a merger or interaction in the past 1–2 Gyrs, and began to be in re-equilibrium (Belsole et al. 2004). Since the gas distribution to the southwestern side of A1750 C appears to be elongated in the direction of A1750 S, and A1750 S is located at the line connecting A1750 C and N, A1750 S can be suspected to be a companion cluster responsible for the past interaction of A1750 C. A1750 S lies at a projected distance of $\sim 1.2 h^{-1} \text{ Mpc}$ from A1750 C, and has a mean radial velocity similar to that of A1750 C. The fact that we cannot find acceptable solutions in the bound region for the two-body model of A1750 N and C, when we use the relative radial velocity between two brightest galaxies in subclusters, may support that A1750 C experienced a

merger or interaction in the past. It is noted that the existence of no acceptable solutions in the bound region may be also due to the wrong assumption of two-body model (e.g., merging with no angular momentum). However, it is difficult to determine whether the interaction between A1750 N and C is similar to an off-axis merging by comparing with simulated X-ray images, because the distortion of X-ray contours is hardly seen.

On the other hand, the past interaction of A1750 C may be related to the other subcluster. There is seen a concentration of galaxies to the east of A1750 C in the galaxy number density map (shown by a dashed ellipse and denoted by ‘E’ in Fig. 4d), though X-ray images do not show any noticeable peaks. The velocity distribution of galaxies in A1750 E is far from Gaussian, and the velocity dispersion and virial mass for A1750 E are abnormally large, indicating that it may not be a genuine subcluster currently. The past interaction of A1750 E with A1750 C is suspected by the facts that the compression of X-ray image is to the direction of east (Belsole et al. 2004), and that A1750 E is much more smoothly connected to A1750 C compared to A1750 S as shown in the galaxy number density map. Interestingly, there is one active galaxy on the line connecting A1750 E and C, and there are two active galaxies (one early type and one late type) just to the northeast in A1750 E. It is difficult to determine whether the activity of the galaxies associated with A1750 E is triggered by a past interaction with A1750 C or not due to the small number of active galaxies.

A1750 E may be also related to A1750 N. The galaxy number density map in Fig. 4(d) shows that A1750 C is largely connected to A1750 N through A1750 E. To account for the velocity information in addition to the spatial distribution, we present the spatial distribution of cluster galaxies with measured velocities in Fig. 12. The radial velocity of southern part of A1750 E is similar to that of A1750 C, and that of northern part of A1750 E is similar to that of A1750 N.

A1750 N is suspected to experience no mergers in the past, but to be weakly interacting with other sources other than A1750 C now. This is consistent with the findings based on XMM-Newton data by Belsole et al. (2004): (1) the X-ray image of A1750 N is elongated along the northeast direction; (2) there is another extended X-ray source just to the north of A1750 N; (3) the gas temperature of A1750 N is uniform; and (4) the cooling flow is not disrupted in the core region of A1750 N. The distribution of galaxies in the number density and spatial-velocity maps (see Fig. 12) indicate that the current interaction/accretion of A1750 N may be related to A1750 E. In addition, if we plot the spatial distribution of the galaxies with $cz \sim 22,500 \text{ km s}^{-1}$ that might be another small group (star symbols in Fig. 12), the spatial distribution of these galaxies is overlapped with the region connecting to A1750 N and A1750 E. In conclusion, A1750 E maybe a subcluster that was partially disrupted during the previous interaction with A1750 C and is currently interacting with A1750 N.

4.3 E+A Galaxies

We could not find any ‘E+A’ galaxies that have strong Balmer absorption lines with no [O II] emission line in either of A168 and A1750. ‘E+A’ galaxies are usually regarded

as post-starburst galaxies that have experienced starbursts within the last Gyr, and the activity has been abruptly truncated. Since they were first discovered in distant clusters (Dressler & Gunn 1983) and were found more in clusters than in the field (Dressler et al. 1999; Poggianti et al. 1999; Tran et al. 2003, 2004), they were supposed to be cluster-related phenomena. However, the local ($z \leq 0.1$) ‘E+A’ galaxies are rarely found in clusters (Dressler 1987), and are usually found in the low density environment such as poor groups and the field (Zabludoff et al. 1996; Quintero et al. 2004; Blake et al. 2004; Goto 2005; Yan et al. 2008). Therefore, their origin and relation with clusters are still debated (Yang et al. 2008). Interestingly, some ‘E+A’ galaxies are found in nearby merging clusters (Coma at $z \sim 0.023$; Poggianti et al. 2004, and A3921 at $z \sim 0.095$; Ferrari et al. 2005), but they do not appear to be related with the current merging event.

However, in some cases, ‘E+A’ galaxies are expected to exist in merging clusters if the increased ram-pressure of ICM can trigger SF activity of cluster galaxies and subsequently quench it. We checked the equivalent width (EW) of H δ absorption lines for all galaxies in Fig. 10. It is found that the maximum values of EW(H δ) are just 1.15 Å in A168 and 1.17 Å in A1750 that are much smaller than the typical criterion (5Å) for ‘E+A’ galaxies. In conclusion, the existence of galaxies with SF/AGN activity and the lack of ‘E+A’ galaxies in A168, may indicate that the galaxy activity is induced by the cluster merger recently, and is not yet quenched. For A1750, the activity of galaxies associated with the merging between two major subclusters might be not yet triggered, since the merging is in the early stage.

5 SUMMARY

We present the results of a study of dynamical state for two merging binary clusters (A168 and A1750) and the activity of cluster galaxies using the SDSS galaxy sample of which redshifts are available in SDSS or NED. Our primary results are summarised below.

(i) We have found the substructures in each cluster, and have investigated the kinematic and photometric properties of the galaxies in the subclusters.

(ii) Using the two-body model analysis and the X-ray data, we have investigated the merger histories of A168 and A1750. Two subclusters in A168 appear to have experienced last encounter about $3.5 h^{-1}$ Gyr ago, and to be now coming together from the maximum expansion of $1.58 h^{-1}$ Mpc about $0.4 h^{-1}$ Gyr ago. Two major subclusters (A1750 C and N) appear to have started interaction and to be coming together for the first time.

(iii) We have found an excess of galaxies with SF/AGN activity in the region between the two subclusters of A168, which might have been triggered by the cluster merger. However, we found no enhanced concentration of blue galaxies at that region, which is consistent with the result in Tomita et al. (1996).

(iv) In A1750, we could not find any galaxies that show strong activity in the region between two subclusters (A1750 N and C), which is consistent with the scenario that they are in the early stage of merging. A1750 E may be a subcluster

that was partially disrupted during the previous interaction with A1750 C and is currently interacting with A1750 N.

(v) We found no ‘E+A’ galaxies in either of A168 or A1750.

In conclusion, the cluster merger appears to trigger the activity of cluster galaxies, and its effect is different depending on the merging stage. Cluster mergers are usually in different stages, and the conditions of ICM and galaxies in these clusters are diverse. Therefore it is needed to study more clusters in different stages of merging to understand the relation between the galaxy activity and the dynamical state of the clusters.

ACKNOWLEDGMENTS

The authors thank the anonymous referee for useful comments that improved significantly the original manuscript. This work was supported in part by a grant R01-2007-000-20336-0 from the Basic Research Program of the Korea Science and Engineering Foundation.

Funding for the SDSS and SDSS-II has been provided by the Alfred P. Sloan Foundation, the Participating Institutions, the National Science Foundation, the U.S. Department of Energy, the National Aeronautics and Space Administration, the Japanese Monbukagakusho, the Max Planck Society, and the Higher Education Funding Council for England. The SDSS Web Site is <http://www.sdss.org/>.

The SDSS is managed by the Astrophysical Research Consortium for the Participating Institutions. The Participating Institutions are the American Museum of Natural History, Astrophysical Institute Potsdam, University of Basel, Cambridge University, Case Western Reserve University, University of Chicago, Drexel University, Fermilab, the Institute for Advanced Study, the Japan Participation Group, Johns Hopkins University, the Joint Institute for Nuclear Astrophysics, the Kavli Institute for Particle Astrophysics and Cosmology, the Korean Scientist Group, the Chinese Academy of Sciences (LAMOST), Los Alamos National Laboratory, the Max-Planck-Institute for Astronomy (MPIA), the Max-Planck-Institute for Astrophysics (MPA), New Mexico State University, Ohio State University, University of Pittsburgh, University of Portsmouth, Princeton University, the United States Naval Observatory, and the University of Washington.

This research has made use of the NASA/IPAC Extragalactic Database (NED) which is operated by the Jet Propulsion Laboratory, California Institute of Technology, under contract with the National Aeronautics and Space Administration.

REFERENCES

- Adelman-McCarthy J. K., et al., 2008, *ApJS*, 175, 297
 Baldwin J. A., Phillips M. M., Terlevich R., 1981, *PASP*, 93, 5
 Beers T. C., Geller M. J., Huchra J. P., 1982, *ApJ*, 257, 23
 Beers T. C., Kage J. A., Preston G. W., Shectman S. A., 1990, *AJ*, 100, 849
 Beers T. C., Gebhardt K., Forman W., Huchra J. P., Jones C., 1991, *AJ*, 102, 1581
 Bekki K., 1999, *ApJ*, 510, L15
 Belsole E., Pratt G. W., Sauvageot J.-L., Bourdin H., 2004, *A&A*, 415, 821
 Blake C., et al., 2004, *MNRAS*, 355, 713
 Blanton M. R., Lin H., Lupton R. H., Maley F. M., Young N., Zehavi I., Loveday J., 2003a, *AJ*, 125, 2276
 Blanton M. R., et al., 2003b, *AJ*, 125, 2348
 Buote D. A., 2002, *ASSL*, 272, 79
 Burns J. O., Roettiger K., Ledlow M., Klypin A., 1994, *ApJ*, 427, L87
 Caldwell N., Rose J. A., 1997, *AJ*, 113, 492
 Caldwell N., Rose J. A., Sharples R. M., Ellis R. S., Bower R. G., 1993, *AJ*, 106, 473
 Castander F. J., et al., 2001, *AJ*, 121, 2331
 Choi Y.-Y., Park C., Vogeley M. S., 2007, *ApJ*, 658, 884
 Cortese L., Gavazzi G., Boselli A., Iglesias-Paramo J., Carrasco L., 2004, *A&A*, 425, 429
 Cortese L., Gavazzi G., Boselli A., Franzetti P., Kennicutt R. C., O’Neil K., Sakai S., 2006, *A&A*, 453, 847
 De Propriis R., et al., 2004, *MNRAS*, 351, 125
 Donnelly R. H., Forman W., Jones C., Quintana H., Ramirez A., Churazov E., Gilfanov M., 2001, *ApJ*, 562, 254
 Dressler A., 1987, *nngp.proc*, 276
 Dressler A., Gunn J. E., 1983, *ApJ*, 270, 7
 Dressler A., Shectman S. A., 1988, *AJ*, 95, 985
 Dressler A., Smail I., Poggianti B. M., Butcher H., Couch W. J., Ellis R. S., Oemler A. J., 1999, *ApJS*, 122, 51
 Fadda D., Girardi M., Giuricin G., Mardirossian F., Mezzetti M., 1996, *ApJ*, 473, 670
 Fasano G., Franceschini A., 1987, *MNRAS*, 225, 155
 Ferrari C., Benoist C., Maurogordato S., Cappi A., Slezak E., 2005, *A&A*, 430, 19
 Forman W., Bechtold J., Blair W., Giacconi R., van Speybroeck L., Jones C., 1981, *ApJ*, 243, L133
 Fujita Y., Takizawa M., Nagashima M., Enoki M., 1999, *PASJ*, 51, L1
 Fukugita M., Ichikawa T., Gunn J. E., Doi M., Shimasaku K., Schneider D. P., 1996, *AJ*, 111, 1748
 Girardi M., Giuricin G., Mardirossian F., Mezzetti M., Boschini W., 1998, *ApJ*, 505, 74
 Girardi M., Biviano A., 2002, *ASSL*, 272, 39
 Gnedin O. Y., 2003, *ApJ*, 582, 141
 Goto T., 2005, *MNRAS*, 357, 937
 Gunn J. E., et al., 1998, *AJ*, 116, 3040
 Gunn J. E., et al., 2006, *AJ*, 131, 2332
 Hallman E. J., Markevitch M., 2004, *ApJ*, 610, L81
 Hogg D. W., Finkbeiner D. P., Schlegel D. J., Gunn J. E., 2001, *AJ*, 122, 2129
 Hwang H. S., Lee M. G., 2007, *ApJ*, 662, 236
 Hwang H. S., Lee M. G., 2008, *ApJ*, 676, 218
 Ivezić Ž., et al., 2004, *AN*, 325, 583
 Jones C., Forman W., 1999, *ApJ*, 511, 65
 Johnston-Hollitt M., Sato M., Gill J. A., Fleenor M. C., Brick A.-M., 2008, *MNRAS*, 390, 289
 Kapferer W., et al., 2006, *A&A*, 447, 827
 Kennicutt R. C., Jr., 1998, *ARA&A*, 36, 189
 Kewley L. J., Groves B., Kauffmann G., Heckman T., 2006, *MNRAS*, 372, 961
 Kronberger T., Kapferer W., Ferrari C., Unterguggenberger S., Schindler S., 2008, *A&A*, 481, 337

- Lupton R. H., Ivezić Z., Gunn J. E., Knapp G., Strauss M. A., Yasuda N., 2002, *SPIE*, 4836, 350
- Markevitch M., Vikhlinin A., 2007, *PhR*, 443, 1
- Martini P., Mulchaey J. S., Kelson D. D., 2007, *ApJ*, 664, 761
- Mathis H., Lavaux G., Diego J. M., Silk J., 2005, *MNRAS*, 357, 801
- Mauduit J.-C., Mamon G. A., 2007, *A&A*, 475, 169
- Miller N. A., Owen F. N., 2003, *AJ*, 125, 2427
- Park C., Choi Y.-Y., 2005, *ApJ*, 635, L29
- Park C., Choi Y.-Y., 2009, *ApJ*, 691, 1828
- Park C., Hwang H. S., 2008, *ApJ*, accepted (*astro-ph/0812.2088*)
- Pier J. R., Munn J. A., Hindsley R. B., Hennessy G. S., Kent S. M., Lupton R. H., Ivezić Ž., 2003, *AJ*, 125, 1559
- Poggianti B. M., Smail I., Dressler A., Couch W. J., Barger A. J., Butcher H., Ellis R. S., Oemler A. J., 1999, *ApJ*, 518, 576
- Poggianti B. M., Bridges T. J., Komiyama Y., Yagi M., Carter D., Mobasher B., Okamura S., Kashikawa N., 2004, *ApJ*, 601, 197
- Poole G. B., Fardal M. A., Babul A., McCarthy I. G., Quinn T., Wadsley J., 2006, *MNRAS*, 373, 881
- Quintero A. D., et al., 2004, *ApJ*, 602, 190
- Ramírez A., Quintana H., 1990, *RMxAA*, 21, 69
- Ricker P. M., 1998, *ApJ*, 496, 670
- Ricker P. M., Sarazin C. L., 2001, *ApJ*, 561, 621
- Schlegel D. J., Finkbeiner D. P., Davis M., 1998, *ApJ*, 500, 525
- Smith J. A., et al., 2002, *AJ*, 123, 2121
- Stoughton C., et al., 2002, *AJ*, 123, 485
- Struble M. F., Rood H. J., 1999, *ApJS*, 125, 35
- Takizawa M., 2000, *ApJ*, 532, 183
- Tegmark M., et al., 2004, *ApJ*, 606, 702
- Tomita A., Nakamura F. E., Takata T., Nakanishi K., Takeuchi T., Ohta K., Yamada T., 1996, *AJ*, 111, 42
- Tran K.-V. H., Franx M., Illingworth G., Kelson D. D., van Dokkum P., 2003, *ApJ*, 599, 865
- Tran K.-V. H., Franx M., Illingworth G. D., van Dokkum P., Kelson D. D., Magee D., 2004, *ApJ*, 609, 683
- Tremonti C. A., et al., 2004, *ApJ*, 613, 898
- Tucker D. L., et al., 2006, *AN*, 327, 821
- Ulmer M. P., Wirth G. D., Kowalski M. P., 1992, *ApJ*, 397, 430
- Uomoto A., et al., 1999, *AAS*, 31, 1501
- Yan R., et al., 2008, *MNRAS*, submitted, (*astro-ph/0805.0004*)
- Yang Y., Zhou X., Yuan Q., Jiang Z., Ma J., Wu H., Chen J., 2004a, *ApJ*, 600, 141
- Yang Y., Huo Z., Zhou X., Xue S., Mao S., Ma J., Chen J., 2004b, *ApJ*, 614, 692
- Yang Y., Zabludoff A., Zaritsky D., Mihos C., 2008, *ApJ*, 688, 945
- York D. G. et al., 2000, *AJ*, 120, 1579
- Zabludoff A. I., Zaritsky D., Lin H., Tucker D., Hashimoto Y., Shectman S. A., Oemler A., Kirshner R. P., 1996, *ApJ*, 466, 104